

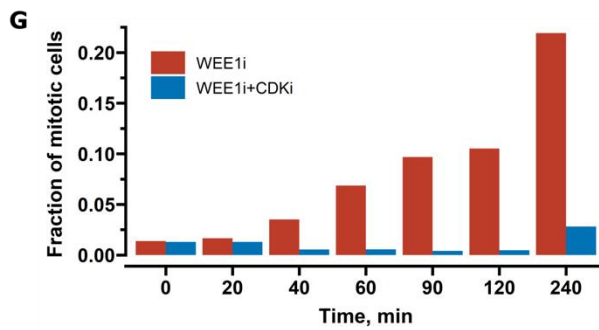
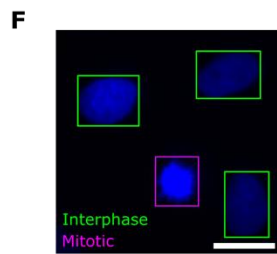
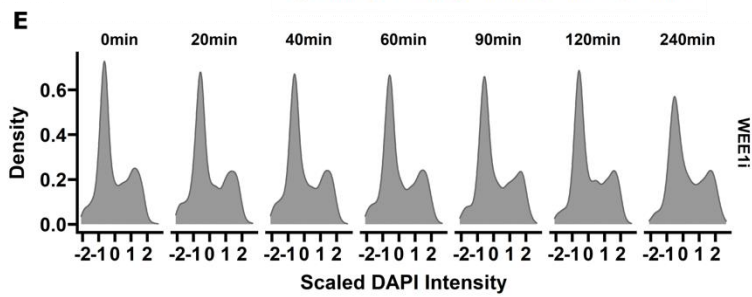
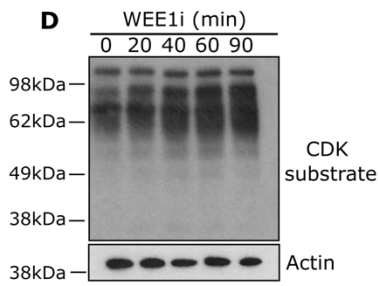
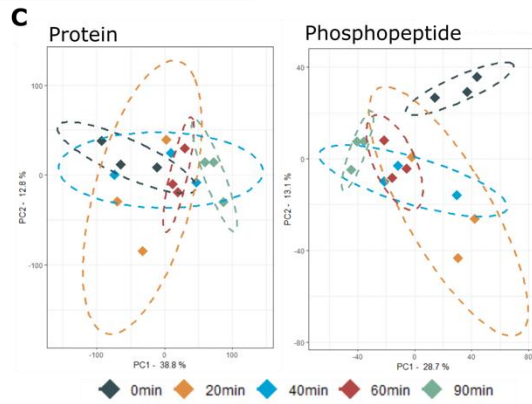
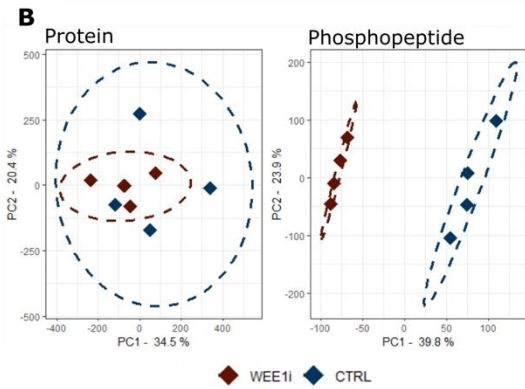
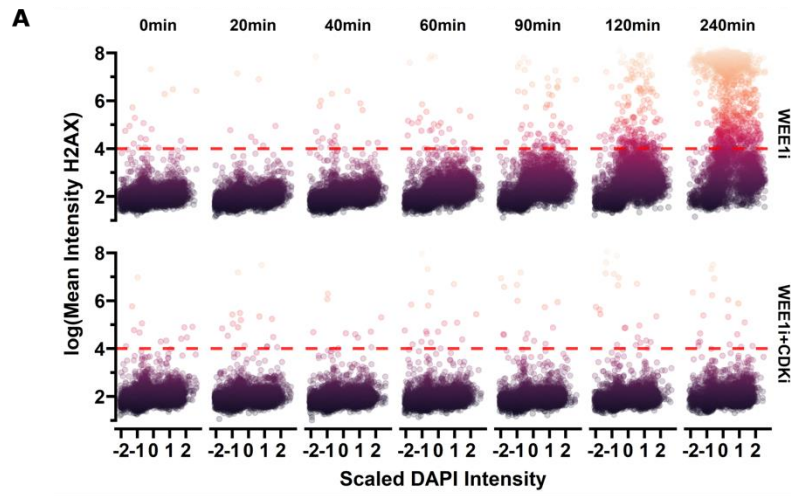
iScience, Volume 26

## **Supplemental information**

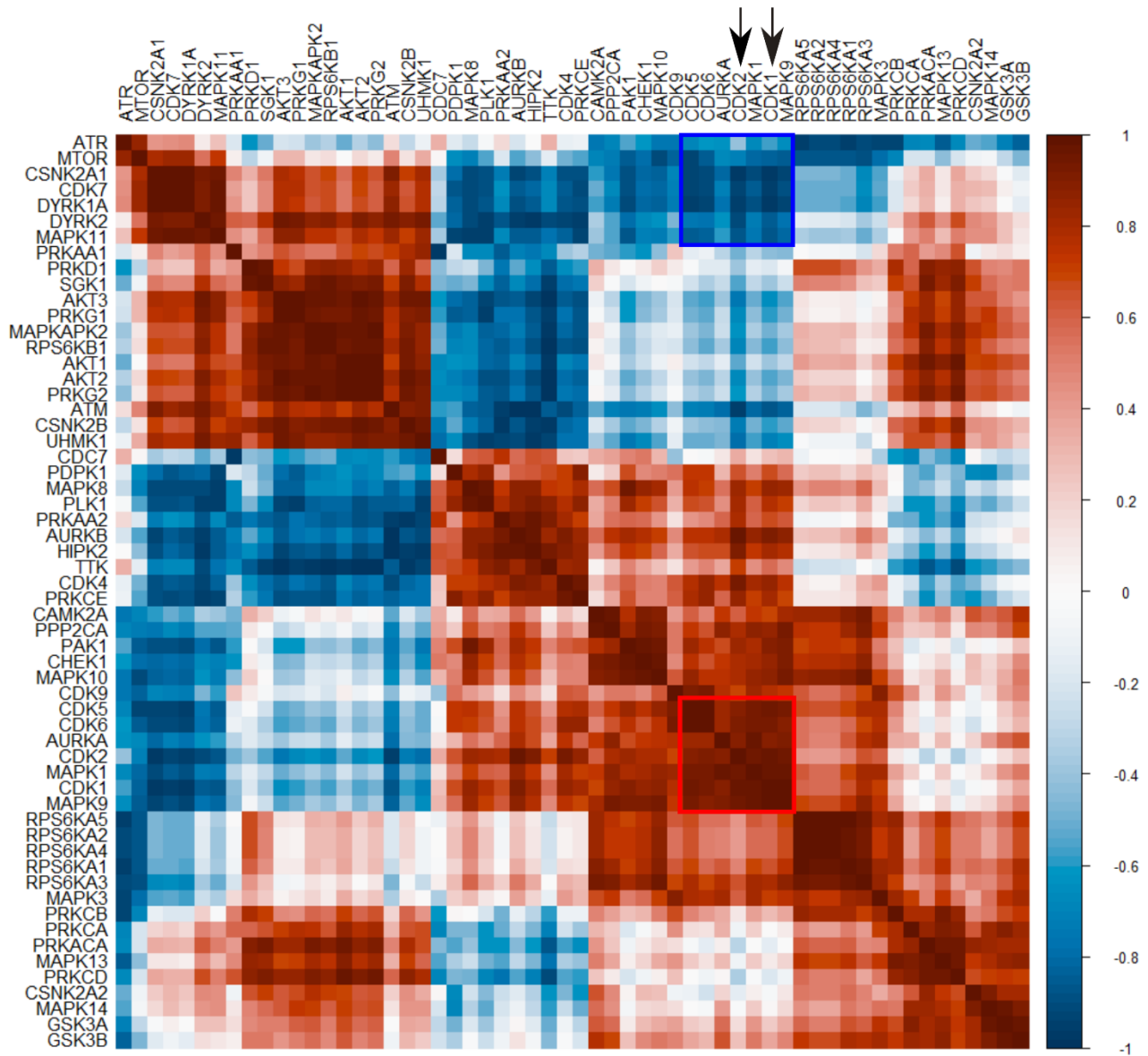
**Temporal phosphoproteomics reveals**

**WEE1-dependent control of 53BP1 pathway**

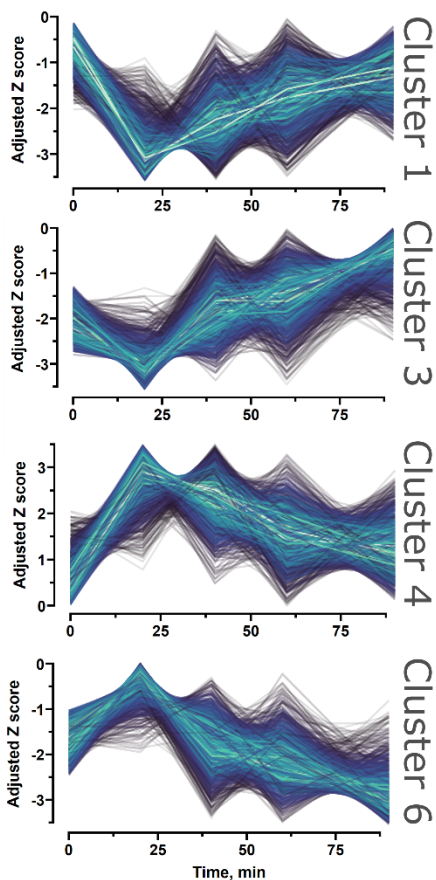
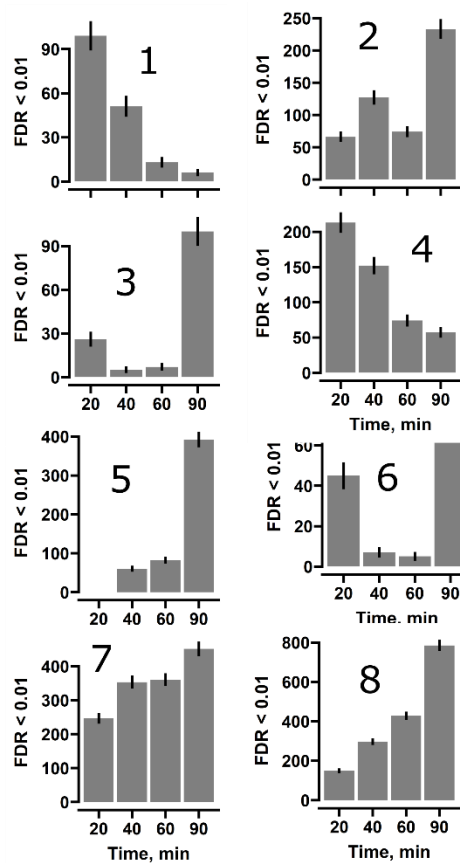
**Valdemaras Petrosius, Jan Benada, Olaf Nielsen, Erwin M. Schoof, and Claus Storgaard Sørensen**



**Figure S1. Time-resolved dynamics of cellular responses to WEE1 inhibition. Related to Figure 1. (A)** Scatter plot showing  $\gamma$ H2AX levels at different timepoints after WEE1 inhibition. CDK inhibitors are used (CDKi) to show that the observed increase in  $\gamma$ H2AX is CDK activity dependent. Scaled DAPI intensity is plotted on the x-axis and the log transformed  $\gamma$ H2AX intensity is on the y-axis. The plots are faceted for different timepoints and treatments. The red dashed line indicated a manually set threshold value above which a cell would be considered damaged. N=1, n>1000. **(B)** Principal component analysis plots of protein and phosphopeptide abundances for the time course experiment. The points are colored by the respective adavosertib treatment duration. Ellipses represent the confidence interval of the clustering. **(C)** Identical to **A**, but for the single timepoint dataset. **(D)** Immunoblot stained with antibodies against total CDK substrate and actin. **(E)** Scaled total DAPI density distribution at different timepoints after adavosertib addition. **(F)** Representative image from QIBC analysis showing the gating of interphase (green) and mitotic-like (red square) cells, based on their morphological features. White scale bar denotes 20  $\mu$ m **(G)** Bar plot showing the cell population fraction of mitotic-like cells at different timepoints after WEE1i inhibition without or with CDK1 inhibition. QIBC and FACS experiments were carried out only once. N=1, n>1000. N indicates the number of times the experiment has been replicated and n notes the minimal amount of cells quantified per condition.



**Figure S2. Kinase activity correlation map following WEE1 inhibition. Related to Figure 2**  
 Relative kinase activity was calculated for each time point for kinases with at least 5 detected substrates. Spearman correlation was then calculated for all possible combinations. Kinases were then clustered with hierarchical clustering to identify the most correlated trends. Color indicates the correlation coefficient. Arrows denote CDK1 and CDK2. Red and blue squares indicated areas of interest in the correlation map.

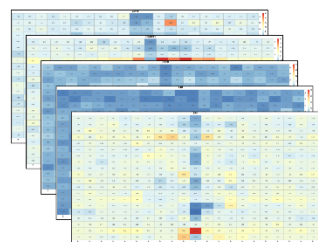
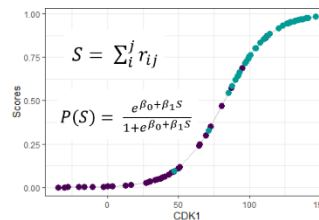
**A****B****C**

21 amino acid motifs from  
ScansitePlus + SIGNOR database  
(curation effort > 2  
motif\_count > 20)

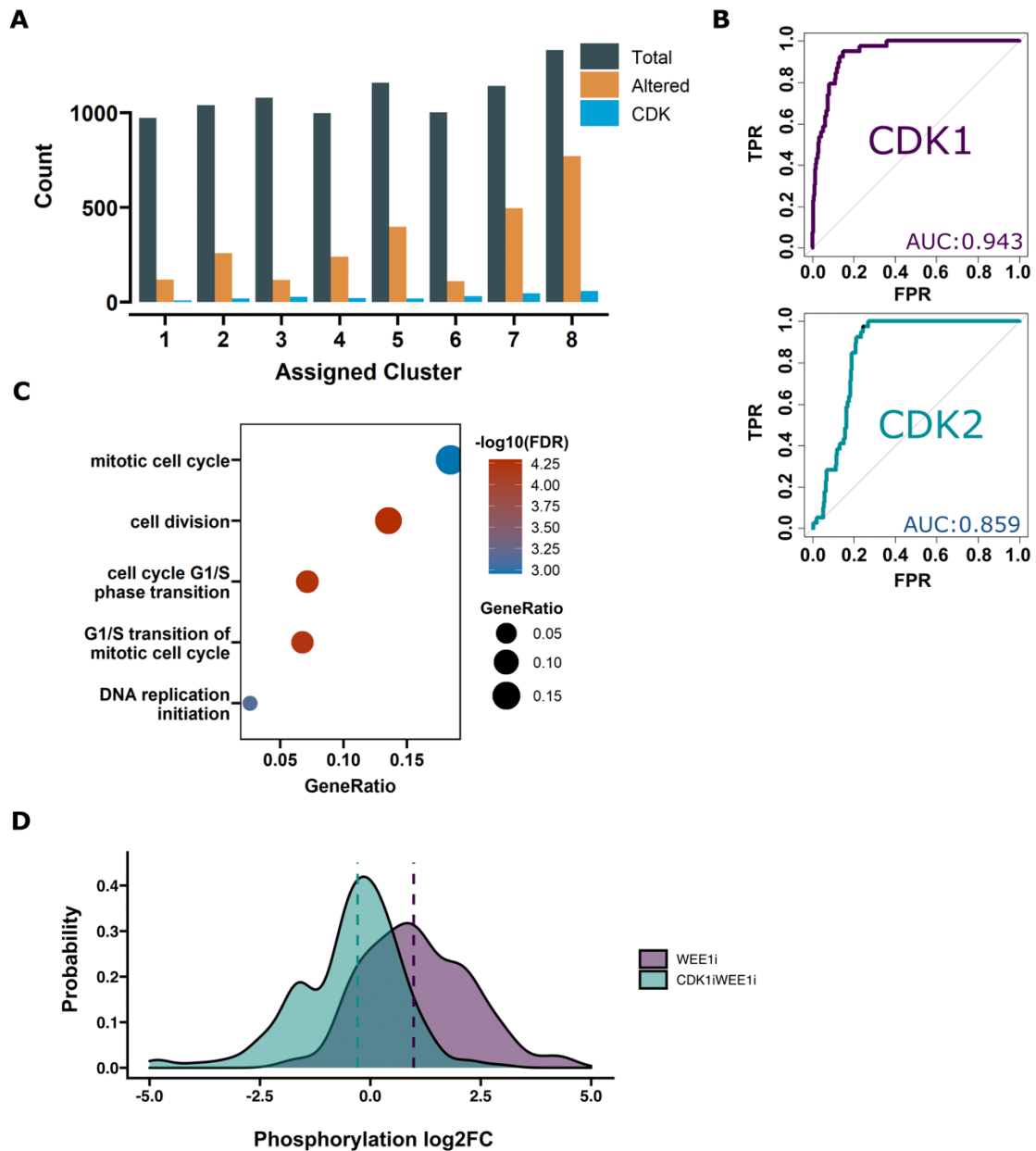
+

Disorder based background  
amino acid probability

$$RS_a(K_a, N, p_a) = -\log_{10} \frac{P_a(k, k \ge K | N, p_a)}{P_a(k, k \le K | N, p_a)}$$

**Data****Model****PSSM****Scoring**

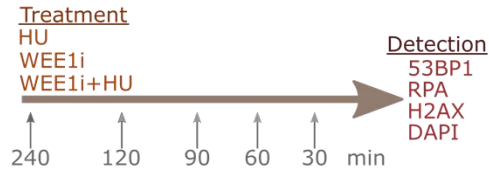
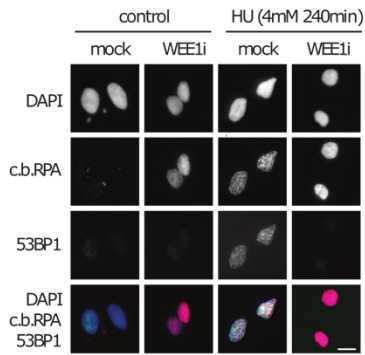
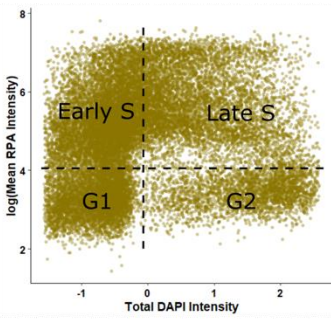
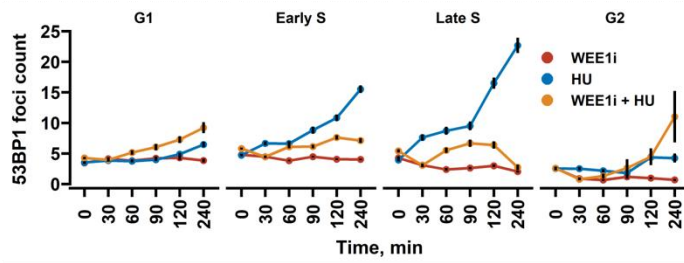
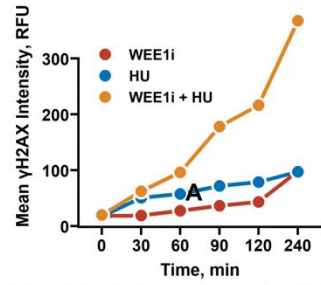
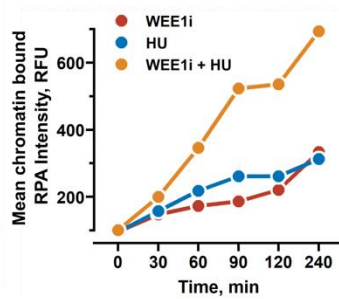
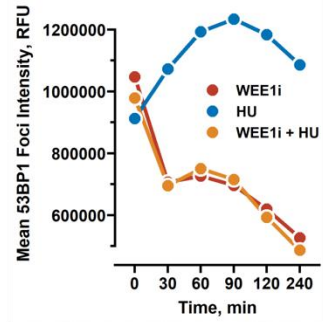
**Figure S3. Fuzzy c-means (FMC) clustering and scheme for PSSM generation. Related to Figure 3 and 4. (A)** The calculated FCM clusters are shown on the left. Each line corresponds to the dynamics of a single phosphorylation site. The z-scores are plotted on the y axis and time on the x axis. Color indicates the probability of the site for the cluster. **(B)** Bar plots showing the number of significant phosphorylation site alterations (FDR < 0.05) in different clusters at different timepoints after adavosertib treatment. Black bars indicate the squared root of the count. **(C)** Scheme of PSSM based scoring of phosphorylation sites. CDK1 and CDK2 phosphorylation sites were extracted from PSP and SIGNOR databases. The background amino acid frequency was adjusted to 0.4 probability of disorder to account for the tendency of phosphorylation site to lie in disordered protein regions. A binomial probability model was then used to calculate the over or underrepresentation scores for each amino acid at every position generating a 20x21 position specific-scoring matrix (PSSM). Logistic regression model was then trained to transform the arbitrary scores into probabilities.



**Figure S4. PSSM based prediction of CDK substrates. Related to Figure 4. (A)** Bar plot showing count for total, altered and CDK sites in FCM clusters. Total sites represent the total number of phosphorylation stratified to the cluster. Altered represents the number of significantly ( $\text{FDR} < 0.05$ ) altered phosphorylation sites in cluster. CDK represent the number of known CDK sites based on PSP and SIGNOR databases. **(B)** Receiver operating characteristic (ROC) curve for CDK1 and CDK2 phosphorylation site prediction based on PSSM scores. The area under the

curve (AUC) is indicated in the bottom right corner. **(C)** Gene-set overrepresentation analysis for biological processes of predicted CDK1 and CDK2 sites. The size of the dots indicates the number of genes found in the cluster and the color indicates the FDR adjusted p-value. **(D)** Density-plot of log<sub>2</sub> transformed fold-changes (log<sub>2</sub>FC) of phosphorylation site abundances after either adavosertib treated (WEE1i) or adavosertib and CDK1i treated (CDK1iWEE1i) compared to control.



**A****B****C****D****E****F****G**

**Figure S5. Cell cycle segmentation and DNA damage marker quantification by QIBC after adavosertib HU treatment. Related to Figure 7. (A)** Experimental set-up schematics for adavosertib and HU (4mM) treatments. **(B)** Representative immunofluorescent images of chromatin bound RPA (c.b.RPA), 53BP1 foci of adavosertib and HU treated cells. Scale bar represents 20  $\mu\text{m}$ . **(C)** Cell cycle segmentation with manually set thresholds (dashed black lines) based on the cell cycle profile. The cell cycle segments are indicated in the plot (G1, early S, late S and G2/M). **(D)** Line plots showing mean 53BP1 foci counts at different time points in segmented cell populations with adavosertib and HU treatment. N=2, n>900; black bars indicate SE. **(E)** Mean  $\gamma\text{H2AX}$  intensity. **(F)** Mean chromatin bound RPA intensity. **(G)** Mean 53BP1 foci intensity. N=2, n>900. N indicates the number of times the experiment has been replicated and n notes the minimal amount of cells quantified per condition.

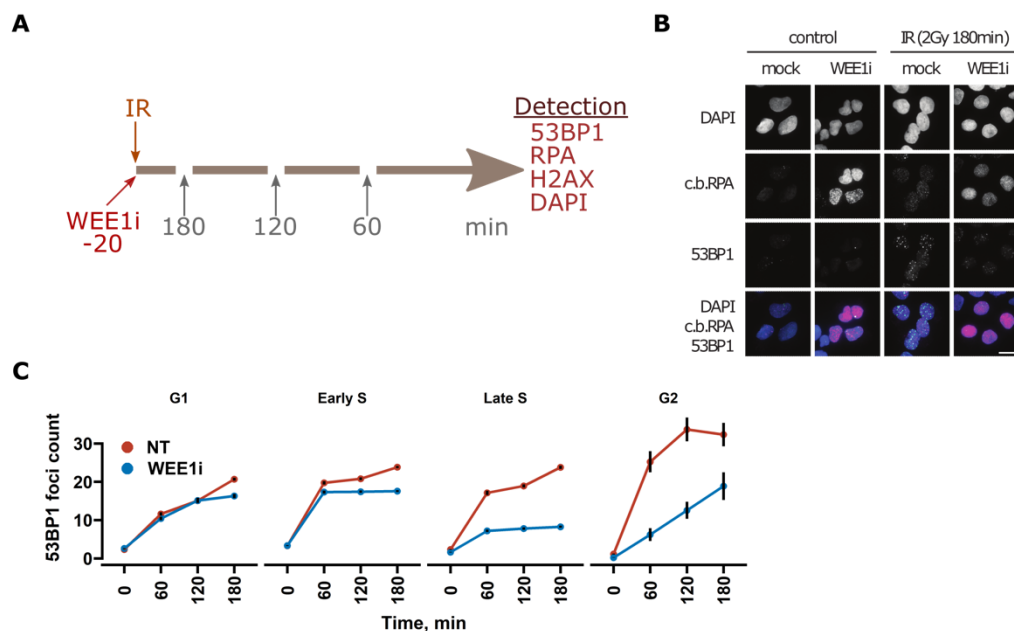
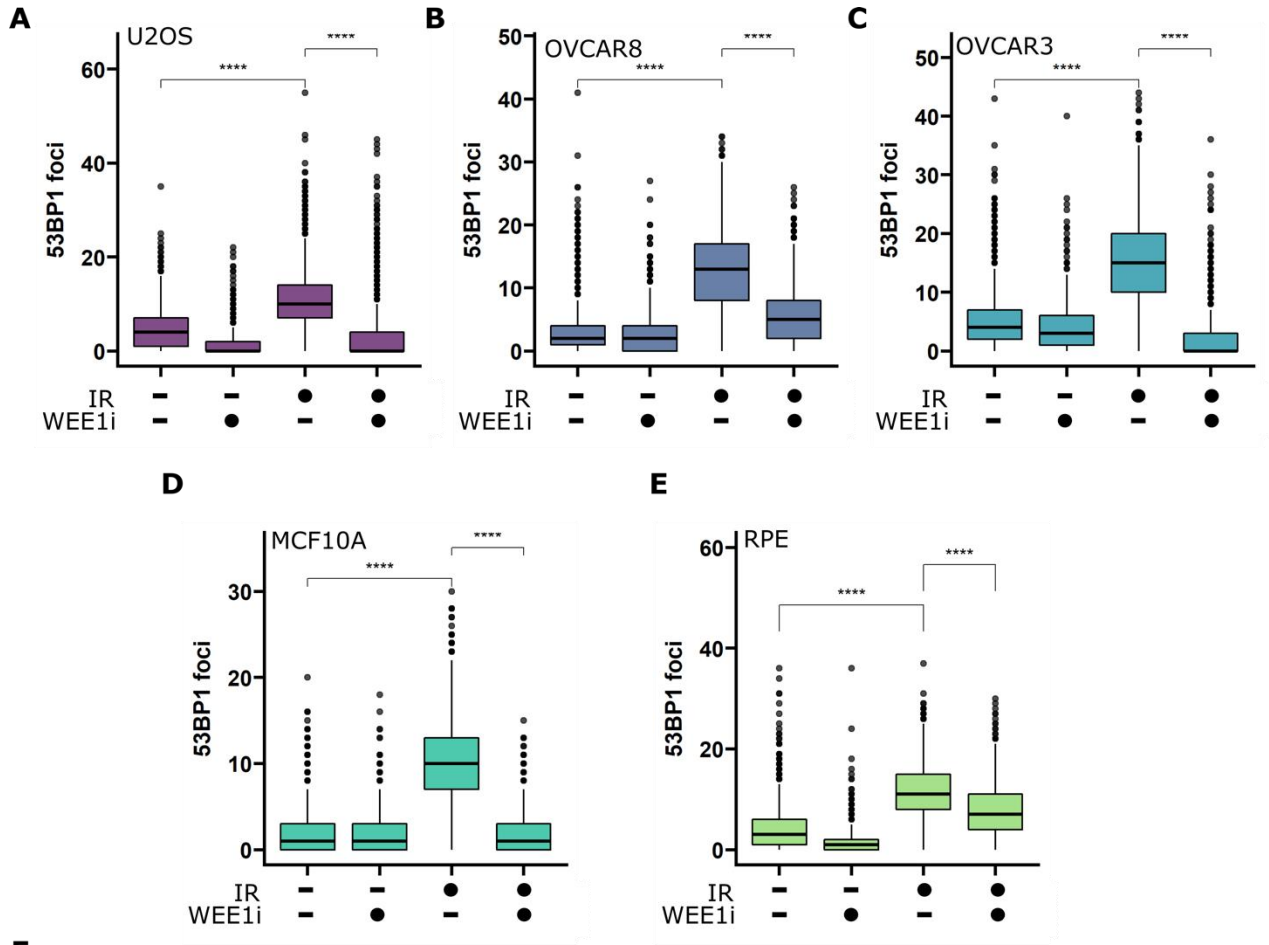
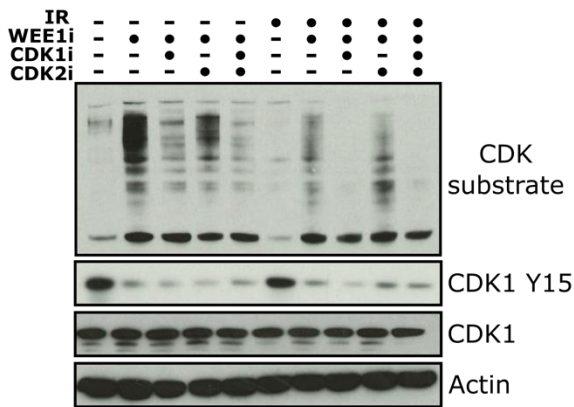


**Figure S6. Cell cycle segmentation and DNA damage marker quantification by QIBC after adavosertib IR treatment. Related to Figure 7. (A)** Experimental set-up schematics for adavosertib and IR (2 Gy) treatments. WEE1 inhibitor (1  $\mu$ M) was added 20 min prior to the irradiation (IR). **(B)** Representative immunofluorescent images of chromatin bound RPA (c.b.RPA), 53BP1 foci of adavosertib and HU treated cells. Scale bar represents 20  $\mu$ m. **(C)** Line plots showing mean 53BP1 foci counts at different time points in segmented cell populations for adavosertib and IR treated cells. All experiments were carried out in triplicate and one representative replicate is shown. N=3, n>1000. N indicates the number of times the experiment has been replicated and n notes the minimal amount of cells quantified per condition. Black bars indicate SE.



**F**



A

**Figure S7 WEE1 inhibition impacts 53BP1 in multiple cell lines. Related to Figure 7. (A-E)** Boxplot of 53BP1 foci in different cell lines. **(A)** U2OS **(B)** OVCAR8 **(C)** OVCAR3 **(D)** MFC10A **(E)** RPE. The cells were treated with 2 Gy of IR radiation without or with WEE1 inhibition and fixed after 4h. P-values were calculated with t.test. \*\*\*\* indicates p-val < 0.0001. **(F)** Immunoblot of whole cell extracts treated with different inhibitors 3h post IR. Antibodies against total CDK substrate, CDKp Y15, CDK1 and actin were used. All QIBC experiments were carried out at least in duplicate and one representative replicate is shown. N=2, n>500. N indicates the number of times the experiment has been replicated and n notes the minimal amount of cells quantified per condition.